CHAPTER IV
REACTIVE PROCESSING OF POLYPROPYLENE – MODIFIED CLAY NANOCOMPOSITES BY CHEMICAL AND PLASMA - ASSITED PROCESSES

4.1 Abstract

We demonstrated the preparation of polypropylene-clay nanocomposites via two reactive processes. The comparison between a physically reactive extrusion in and a chemically reactive processing was investigated. Prior to mixing with polypropylene matrix, the bentonite was functionalized with γ-methacryloxypropyltrimethoxysilane (MPS). XRD pattern showed an expanded interlamellar space of MPS-functionalized bentonite. The modified bentonite was mixed with polypropylene to obtain polymer-clay nanocomposites. As for the plasma-based nanocomposites, a plasma treater was utilized for preparing the plasma-treated melt extrudates of PP-clay nanocomposites. The latter process is relavant to a chemical initiator. Dicumyl peroxide was useful for the fabrication of the nanocomposites via a chemical reaction. A field emission scanning electron microscope coupled with energy dispersive X-ray spectrometer (FE-SEM/EDS) was used for observing the dispersion of clay in the nanocomposites. A thermogravimetric analyzer (TGA) was utilized to investigate the thermal stability of them. XRD was used for determining the crystal structure of nanocomposite films. Moreover, the solvent extraction technique was used to determine the interfacial interaction between PP and clay. With the reactive processing, the FE-SEM illustrated the better distribution and dispersion of clay in the PP matrix, the XRD patterns showed the partial intercalation of PP chains into the interlayer of bentonite, and TGA analysis exhibited the improved thermal stability. From solvent extraction by xylene, the nanocomposites prepared by a plasma generator provided the highest amount of residue and manifested the highest thermal stability resulting from the favorable interface (strong interaction) between the polymer chains and the filler.

Keywords: Clay, Initiator, Nanocomposites, Plasma, Polypropylene

4.2 Introduction

Polymer-clay nanocomposites have enticed the attention of researchers with thanks to their remarkable properties (Maria *et al.*, 2011). Typically, addition of a few amount of clay (usually not exceeding 5 wt.%) (Azizi *et al.*, 2010) to polymer may enhance mechanical and thermal properties of nanocomposites originating from the platelet structure with high aspect ratio of clay in nano-scale dispersion (Sharma *et al.*, 2009).

Polypropylene (PP), one of the major commodity plastics, is widely used in several engineering and biomedical applications. Among all thermoplastics, it offers best performance and low cost (Tang *et al.*, 2003).

Bentonite is a member of smectite clay, which is a layered aluminium silicate with exchangeable cations and reactive OH groups on the surface. Since bentonite is hydrophilic, it is not compatible with most polymers and must be chemically modified to render its surface more hydrophobic (Ray and Okamoto, 2003).

In this research, both silanation process using silane coupling agents and reactive processing by plasma and peroxide are chosen for compatibility enhancement. Silane coupling agents are used to enhance the adhesion of organic resins to inorganic surfaces in composite materials contributing to improvements in nanocomposite properties. In order to meet the requirement of green process, researchers have been searching for other technologies for the reactive manufacturing in place of chemical initiators.

Plasma is, therefore, one of alternatives for a reactive processing, enhancing the grafting of silane on polymer via physical treatment (Xie *et al.*, 2010). In this work, a plasma generator is employed for initiating free radical grafting reaction of silane-modified clay and PP during the melt state compared to the use of reactive ingredient, dicumyl peroxide (DCP) during the melt-compounding process in the extruder. Consequently, the grafting gives rise to an increase in interfacial strength of the polymer-clay nanocomposites (Xie *et al.*, 2010). Plasma is clean and dry process, produced by high voltage and the close proximity of two electrodes at standard atmospheric pressure. Their advantages are ease of use, no requirements of damaging

solvents, enhancement of adhesion, and initiating crosslinking and grafting in particular (Nehra *et al.*, 2008).

Generally, there are several papers on studying the preparation of polymer/clay nanocomposites using silane coupling agents (Liu *et al.*, 2008; Kim *et al.*, 2010; Wan *et al.*, 2008; Wang *et al*, 2007) and peroxides (Mishra and Luyt, 2008; Sun and Chen, 2007) yet few publications have been found concerning the fabrication of nanocomposites using physical crosslinking (Tang *et al.*, 2003; Xie *et al.*, 2010), especially a plasma process.

The aim of this work is to enhance the delamination and dispersion of modified bentonite in polypropylene matrix without resort to compatibilizers by using a plasma technique compared to a chemical initiator using dicumyl peroxide initiator and also to improve the thermal stability of polypropylene/clay nanocomposites by incorporating the modified bentonite. To determine the crystal structure of clay and dispersion of clay in PP matrix, XRD and FE-SEM/EDS were employed, respectively. TGA and DSC were used for the determination of thermal behavior of nanocomposites. Importantly, so as to ascertain whether the interfacial adhesion between the modified clay and PP matrix or not, the solvent extraction by boiling xylene was used to complete dissolve the homopolymer of PP (ungrafted with bentonite) out.

4.3 Experimental Procedures

4.3.1 Materials

Commercial sodium activated bentonite Mac-Gel® (GRADE SAC), Na-BTN, with cationic exchange capacity (CEC) of 49.74 meq/100 g clay and surface area of 31.0 m^2/g, supplied by Thai Nippon Chemical Industry Co., Ltd. Thailand, was purified before use. Commercial polypropylene (PP) under trade name 2300K (MFI 4 g/10 min) supported from T.H.I. Industry Co., Ltd. was used as received. Dicumyl peroxide (DCP), CAS NO. 80-43-3 was purchased from Aldrich and used as received. γ-methacryloxypropyltrimethoxysilane(MPS), CAS NO. 2530-85-0, was purchased from Aldrich and used as received. Absolute ethanol (C_2H_5OH), AR grade, CAS NO. 64-17-5, glacial acetic acid (CH_3COOH), RCI premium grade,

CAS NO. 64-19-7, and xylene ($C_6H_4(CH_3)_2$), AR grade CAS NO. 1330-20-7 were purchased from RCI Labscan and used as received, respectively.

4.3.2 Preparation of Purified Clay

The sodium bentonite clay was first vigorously stirred into a deionized water at 700 rpm overnight by a mechanical stirrer. After that, the supernatant (swollen clay) was separated by centrifugation at 10,000 rpm for 15 minutes and lastly dried, sieved by mesh#400 and kept in a dessiccator before use.

4.3.3 Modification of Bentonite

1.5 wt.% of MPS solution was prepared in 70 vol.% of ethanol aqueous solution pH 4 adjusted by glacial acetic acid and then stirred for 45 min of hydrolysis to silanol. 50 g of bentonite were added respectively into MPS solution. The mixture was stirred at 110 °C for 24 hrs. The plenty of absolute ethanol was used for the removal of excessive MPS during suction filtrating and the modified clay was finally dried at 80 °C in vacuum oven for 5 hrs. The clay was sieved by mesh#400 and kept in a desiccator prior to use.

4.3.3 Preparation of PP-Clay Nanocomposites

The PP and modified clay (SBEN) were mixed in the co-rotating twin-screw extruder (Labtech types LTE-20-32 & LTE-20-40 screw diameter 20 mm) with L/D ratio 40:1, named "PPC-MPS". The operation temperature was performed at 100, 180, 185,190, 190, 190, 190, 195, 200, and 200 °C from hopper to die, respectively and the screw speed at 10 rpm. Secondly, the PP and modified clay were mixed in the same co-rotating twin-screw as well as at the same screw speed and processing temperatures as the former does. After exiting die, the extrudate of nanocomposites was immediately treated by the plasma generator (PT-1 PLASMA TREATER) operated at 6 kV and 10 kHz for 5 sec at the distance of 4 cm from its nozzle to the extrudate, so-called "PPC-PLASMA". Meanwhile, the others called "PPC-0.1DCP, PPC-0.2DCP, and PPC-0.3DCP" represented the nanocomposites which were prepared by mixing PP, modified clay including 0.1, 0.2, 0.3 phr of DCP in the same extruder at the same processing temperatures and screw speed as the plasma-based process was previously carried out. In conclusion, the formulations of nanocomposites designed in this procedure are reported in the Table 4.1.

Table 4.1 Designing formulations of nanocomposite compounds

SAMPLE CODE	PP (wt%)	Modified Bentonite (wt%)
PP	100	-
PPC-MPS	95	5
[1] **PPC-PLASMA**	95	5
[2] **PPC-0.1DCP**	95	5
[3] **PPC-0.2DCP**	95	5
[4] **PPC-0.3DCP**	95	5

[1] prepared by the plasma process

[2, 3, and 4] prepared by the chemical process

4.3.4 Characterizations

4.3.4.1 Melt Flow Index (MFI) Tester

4.3.4.2 Fourier Transform Infared Spectrometer (FT-IR)

The functional group of sodium bentonite and modified bentonite were identified by Nicolet Nexus 670 FT-IR spectrometer. FT-IR was carried out in the transmission mode with 64 scans between 4000 - 400 cm^{-1} at a resolution of 4 cm^{-1}.

4.3.4.3 X-ray Diffractometer (XRD)

The crystal structure of bentonite and modified bentonite was analyzed by a Bruker AXS model Diffractrometer D8with Ni-filtered Cu Kα radiation operated at 40 kV and 30 mA. The experiment was performed in the 2θ range of 5 – 10 degrees with scan speed 2 degree/min and scan step 0.01 degree.

4.3.4.4 Field Emission-Scanning Electron Microscope

The dispersion of bentonite in polymer matrix was determined by using an FE-SEM (HITACHI, S-4800) coupled with energy dispersive X-ray spectrometer (FE-SEM/EDS). The selected samples were dipped and fractured in

liquid nitrogen. Then the samples were sputtered with platinum before observing under an FE-SEM operating at 20 kV.

4.3.4.5 Thermogravimetric analysis (TGA)

The samples were analyzed by TGA using a Perkin-Elmer Pyris Diamond TG/DTA instrument under nitrogen flow of 200 mL/min. The heating process was conducted from 30 - 800°C at a rate of 10°C/min.

4.3.4.6 Differential scanning calorimeter (DSC)

The crystallization and melting behaviors of the active films were measured with a Mettler Toledo, DSC 822e analyzer. All operations were performed under a nitrogen atmosphere. The samples were first heated from 30°C to 200°C at a heating rate of 10°C/min in order to eliminate the influence of thermal history and then cooled down at a rate of 10°C/min from 200°C to -50°C to observe the melt crystallization behavior (1^{st} run) and lastly heated up from -50°C to 200°C at a heating rate of 10°C/min so as to observe the melt behavior (2^{nd} run). The crystallization temperature (T_c) of each specimen was recorded from the first run while its melting temperature (T_m) was collected from the second run.

4.3.4.7 Solvent Extraction

A series of PP-clay nanocomposites based on 5 wt% of modified clay with three different preparation methods, was selected to study the confinement effects on the macroscopic/bulk properties of these nanocomposites using a solvent extraction technique. Each of small pieces of pure PP and PP-clay nanocomposites was weighted (~ 3 g) and placed in a cellulose extraction thimble. The obtained sample was extracted with boiling xylene at 220 °C in a Soxhlet extractor for 24 hours. The material was further dried in a vacuum oven at 70 °C for 24 hours until reaching a constant weight. The macroscopic/bulk properties of xylene soluble and insoluble fractions were investigated and compared with those of starting materials (polymer, clay, and nanocomposites). The change of polymer properties to different morphologies (confinement effects) and thermal analysis were investigated as following and the results are reported in this chapter.

4.4 Results and Discussion

4.4.1 Characterization of Modified Bentonite by FTIR, XRD and TGA

In order to confirm the success of modification of bentonite, the FT-IR spectra of bentonite before and after silanation need comparing. The spectra of bentonite and modified bentonite (Fig.1) show a strong band around 3600 cm^{-1} attributed to the stretching of hydroxyls bonded to the aluminum and magnesium and of strong band around 3400 cm^{-1} corresponding to trapped water molecules (Maria *et al.*, 2011; Rodriguez *et al.*, 1999).

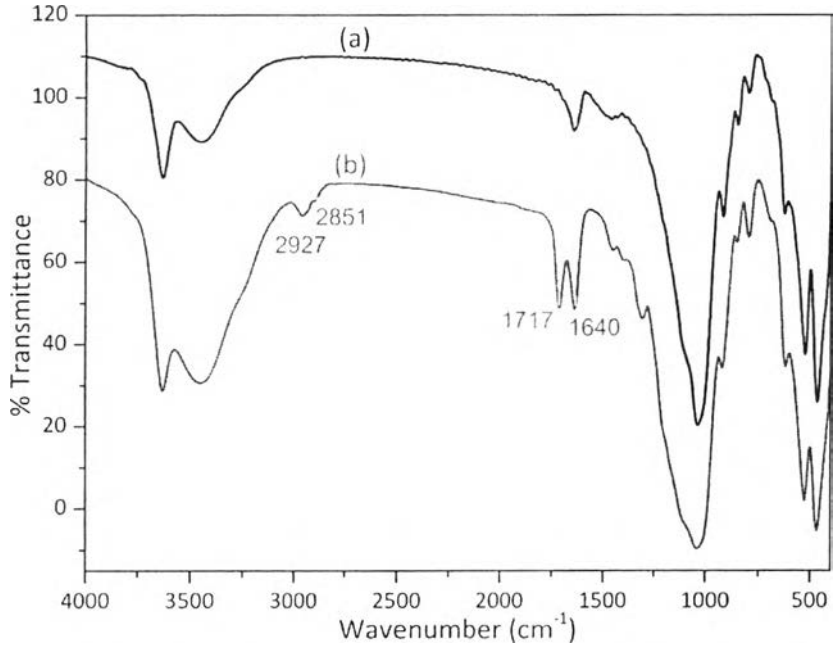

Figure 4.1 FT-IR spectra of (a) BEN and (b) MBEN.

The medium sharp band at 915 and 845 cm^{-1} are assigned to Al-Al-OH and Al-Mg-OH bonds, respectively (Żymankowska-kumon *et al.*, 2012). The absorption bands at 623 and 525 cm^{-1} are because of Al–O–Si bending vibrations (Żymankowska-kumon *et al.*, 2012) as well as the sharp band at 467 cm^{-1} is attributed to Si–O–Si bending vibrations (Zhirong *et al.*, 2011). The very strong

absorption band at 1040 cm^{-1} is due to Si–O bending vibration (Rodriguez *et al.*, 1999).

The spectrum of modified bentonite shows new bands which are not appear in the unmodified bentonite. The absorption signals at 2927 and 2851 cm^{-1} are due to the stretching vibrations of aliphatic hydrocarbon (CH bonds; CH_3 and CH_2) introduced by the organosilane (Maria *et al.*, 2011; Rodriguez *et al.*, 1999; Zhirong *et al.*, 2011). The new bands at 1717 and 1640 cm^{-1} correspond to the stretching vibrations of C=O and C=C groups, respectively as well as the peaks around 1000 cm^{-1} are related to bending vibrations of Si-O-C bonds (Rodriguez *et al.*, 1999).

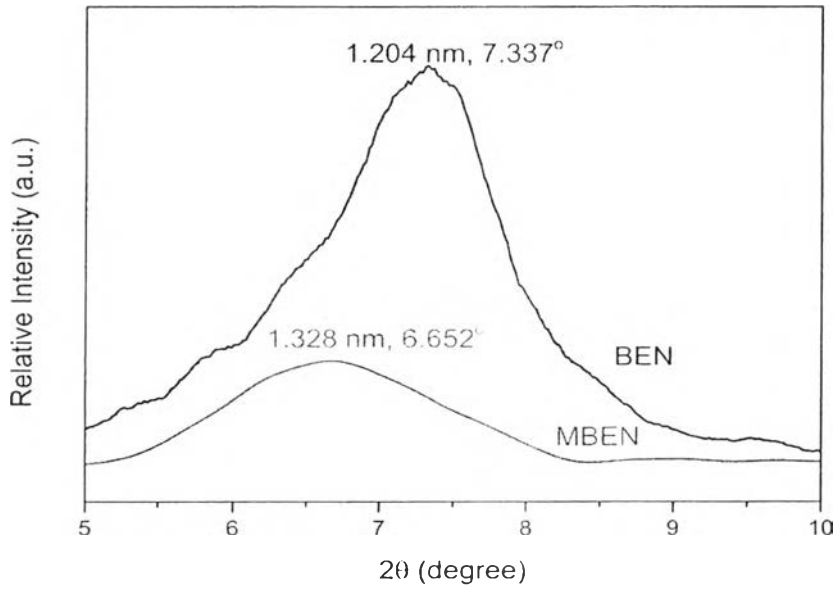

Figure 4.2 XRD patterns of bentonite before and after modification with MPS.

The spectrum shows a shift of characteristic peak (001) from 7.337° to 6.652° corresponding to a change in the basal spacing d_{001} from 1.204 to 1.328 nm. The increase of basal spacing indicates that the organosilane is partly intercalated into the intergalleries of clay after modification (Maria *et al.*, 2011; Joo *et al.*, 2008). However, the interlayer distance d_{001} of Bentonite and MPS-Bentonite are almost identical. This similar phenomenon was also observed by Joo *et al.* They assumed that the organosilane mainly reacted with clay on the outside of clay layers

since the silanol groups mostly situated on the edges of the clay layers rather than on the plane surface of clay (Joo *et al.*, 2008).

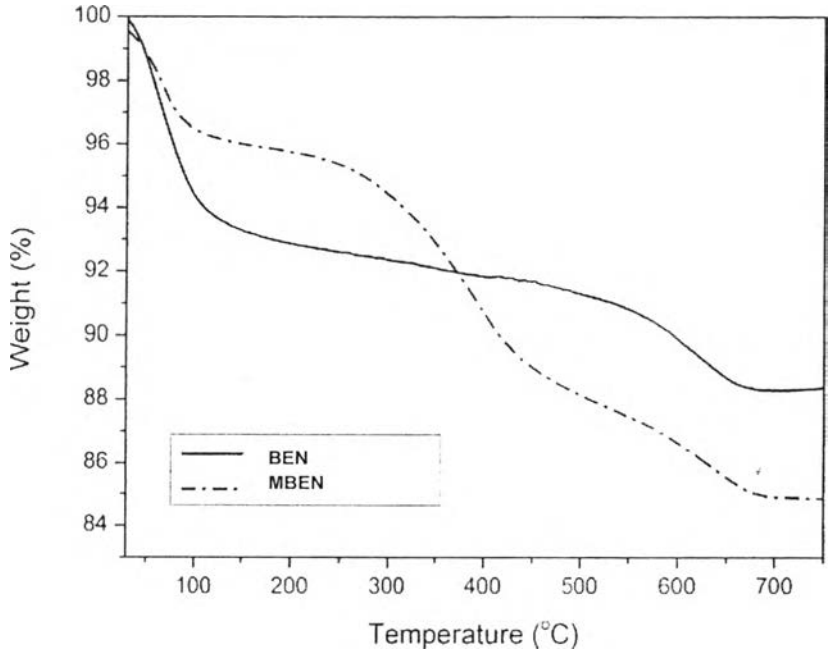

Figure 4.3 Thermogravimetric analysis of bentonite and organosilane-modified bentonite.

The TGA curves of bentonite and modified bentonite were shown in the Fig. 4.3. It is evident that, after modification of bentonite, there is a new step of weight loss taking place in the range of 200 – 600 °C corresponding to the combustion of the silane molecules adsorbed on the clay surface and also to the elimination of hydroxyl groups of the clay (Maria *et al.*, 2011; Rodriguez *et al.*, 1999). The percentage of weight loss indicates the amount of silane grafted on the surface of clay calculated as follows (Maria *et al.*, 2011):

$$\% \text{ Silane grafted amount} = \frac{100 \times W_{200\text{-}600}}{100 - W_{200\text{-}600}} \qquad \text{(Eq. 4.1)}$$

, where $W_{200\text{-}600}$ is the mass loss of organosilane molecules between 200 and 600 °C.

According to Eq. 4.1, the percentage of silane grafted is 8.81% in modified bentonite. Moreover, this graph demonstrates an increase in thermal stability of modified bentonite owing to the presence of organosilane as seen from

the onset decomposition temperature of bentonite presenting a temperature increase of 30 °C, which is consistent with the results obtained by Maria *et al.* (2011).

4.4.2 Determination of Melt Flow Index (MFI) of Virgin PP and PP-Clay Nanocomposites by Melt Flow Index Tester

Table 4.2 Melt Flow Index (MFI) of neat PP and PP-clay nanocomposites at 210 °C

Sample	MFI (g/10 min)
PP	3.700 (0.097)[a]
PPC-MPS	4.935 (0.036)
PPC-PLASMA	4.128 (0.011)
PPC-0.1DCP	10.970 (0.178)
PPC-0.2DCP	12.680 (0.188)
PPC-0.3DCP	21.470 (1.195)

[a] Standard deviation of MFI measurement

The Table 4.2 demonstrates the melt flow index results of PP-clay nanocomposites prepared by different reactive processes which are a plasma technique and various contents of dicumyl peroxide initiator. The nanocomposites without a reactive step and neat PP were used as references for the determination the influence of reactive steps on the melt flowability and processability of the nanocomposites. In this research, it was due to the limitation of the operating condition of the plasma treater, in which the frequency of the machine was fixed at 10 kHz by the manufacturer and plasma voltages were insignificantly different to be varied for comparing the different factors from the machine. Therefore, the plasma condition was maximally set up at 6 kV and 10 kHz for the online reactive processing by the plasma treater. Concurrently, the contents of DCP were run from 0.1 to 0.3 phr in the twin screw extruder. The increasing contents of the DCP greatly influenced on the increase in melt flow index. The higher MFI reflects the lower molecular weight of PP chains resulting from highly severe chain scission from the organic peroxide initiator. These overload chain scission may have detrimental effect

on the degradation of mechanical property of the resultant nanocomposites. Conversely, in the case of the plasma method, the PPC-PLASMA nanocomposites showed the lower MFI compared to other nanocomposites on the ground of chain scission contributing to the grafting reaction taking place by the plasma treater, which reflected the higher viscosity of the nanocomposites. Therefore, the plasma as previously described condition will be employed for the nanocomposites because it provides an optimum grafting result for the preparation. In the next experiment, the further comparison on the performance of the plasma process and 0.1 phr of the chemical initiator will be carried out in order to clarify the validity of reactive process.

4.4.2 Determination of Dispersibility of Modified Bentonite in PP matrix by an FE-SEM/EDS

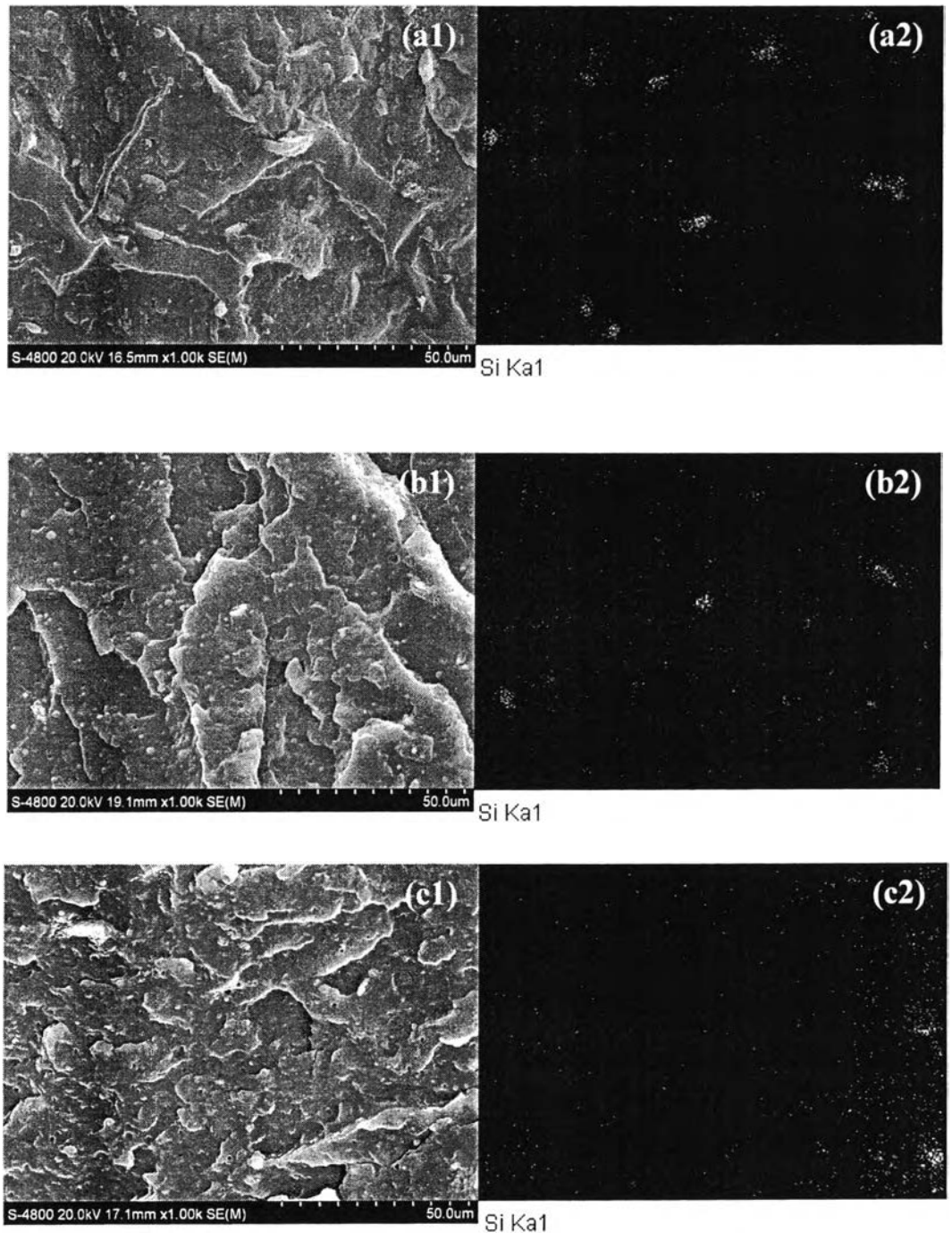

Figure 4.4 FE-SEM micrographs of nanocomposites of (a) PPC-MBEN, (b) PPC-PLASMA, and (c) PPC-0.1DCP.

Figure 4.4 shows the FE-SEM micrographs and Si-mapping images of PPC-MPS, PPC-PLASMA, and PPC-0.1DCP. In the mapping, the white spots indicate the silicon dispersion in the nanocomposites. From the micrographs, they show good distribution of clay layers in the PP matrix but there are some aggregates still occur. With the potential use of reactive processes by plasma and/or organic peroxide, the aggregates are smaller than the nanocomposites without reactive step. Furthermore, it is clearly seen that the dispersion of modified clay in PP is more uniform by plasma reactive step (4.4-b2) than by the chemical initiator (4.4-c2). This effect was suggested by Mishra *et al.* (2008). Such plasma and peroxide treatment seemed to have influence on delamination and dispersion of clay in the polymer matrix as a result of grafting between the clay and polymer, or crosslinking of the polymer (Mishra and Luyt, 2008; Tasanatanachai and Magaraphan, 2007).

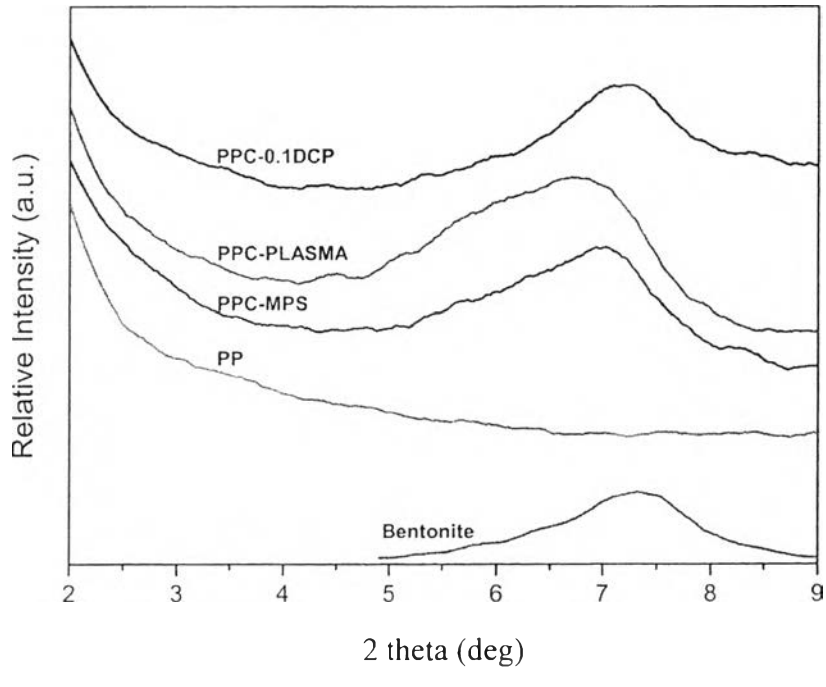

Figure 4.5 XRD patterns showing the crystallographic structure of pristine bentonite, virgin PP, and partially intercalated structures of PPC-MPS, PPC-PLASMA, and PPC-0.1DCP nanocomposite films.

Table 4.3 2-theta angle and d-spacing of clay interlayers in pristine bentonite and after introduction in PP matrix by different approaches

Sample	2-theta (deg)	d-spacing (Å)
Bentonite	7.34	12.0
PP	-	-
PPC-MBEN	6.92	12.8
PPC-PLASMA	6.52	13.6
PPC-0.1DCP	7.12	12.4

The XRD analysis was performed in order to confirm the formation of intercalated/exfoliated nanocomposites. Figure 4.5 depicts the XRD diffragtograms for all the nanocomposites, as well as Table 4.3 manifests their 2-theta angles and d-spacing. For PP-modified clay nanocomposites manufactured by the plasma, it obviously show the highest d-spacing of interlamellar space of modified bentonite compared to pristine bentonite and other nanocomposites, evidently confirmed by A very little shift from 7.34° to 6.52° is congruent with an increase in d-spacing from 1.20 to 1.36 nm. With addition of plasma treater, the reactive extrusion promotes the partially diffusion of the polymer into the interlayers of bentonite because of the formation of favorable interface between clay and polymer which originates from the grafting or crosslinking of free radical species (Tasanatanachai and Magaraphan, 2007) taking place during treating in consonance with the better desirable interface of the inorganic filler and PP matrix in the FE-SEM image (Figure 4.4-b1) and the high extent of clay dispersion in PP matrix as evident from Si-mapping pictures (Figure 4.4-b2).

4.4.3 Thermal analysis

TGA thermograms for the PP and its nanocomposites are summarized in Figure 4.6 and Table 4.4. It is clearly seen in TGA curves that the onset decomposition temperatures are increased in nanocomposites. Importantly, in the case of using the plasma, it is obviously evident that the thermal decomposition temperatures at 2%wt. loss show a marked increase of around 20 °C compared to neat PP in compliance with data attained by Tang *et al.* (2003) and Varothai *et al.* (2007). They suggested that the improvement of degradation temperature of nanocomposites was due to the presence of metal oxides in the modified bentonite such as silica, aluminium, and magnesium (Xie *et al.*, 2010; Varothai *et al.*, 2007).

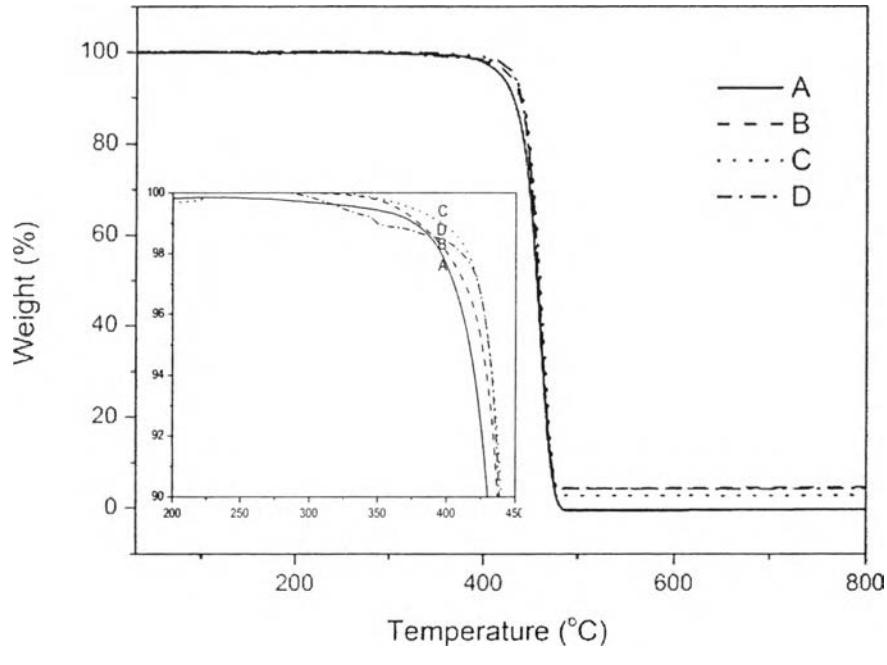

Figure 4.6 Thermogravimetric thermograms of (A) neat PP and its nanocomposites: (B) PPC-MPS, (C) PPC-PLASMA, and (D) PPC-0.1DCP.

Table 4.4 Thermal behavior of neat PP and PP-clay nanocomposites

Sample	T_d onset (°C)	T_d at 2%wt loss (°C)	Char Residue (%)
PP	439.3	395.5	-
PPC-MPS	442.4	399.6	4.4
PPC-PLASMA	444.1	415.2	2.7
PPC-0.1DCP	440.6	410.7	4.1

4.4.4 Fractionation of PP-clay nanocomposites by solvent extractions

To investigate the structural stability and the role of the interfacial interactions between the clay and polypropylene, this solvent extraction technique was performed (Li *et al.*, 2003; Muksing, 2011; Passaglia *et al.*, 2001 and 2008). This study used xylene to separate free polypropylene chains out from the polymer nanocomposite samples. The insoluble part should contain silicate layers strongly bound to PP chains via the reaction to MPS as shown in Figure 4.7 (a) and (b) (Marquez *et al.*, 2005).

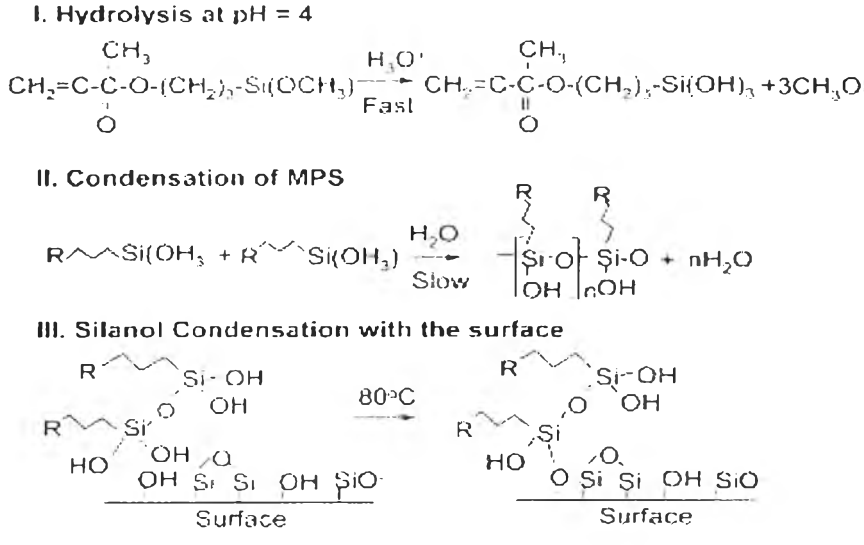

(a)

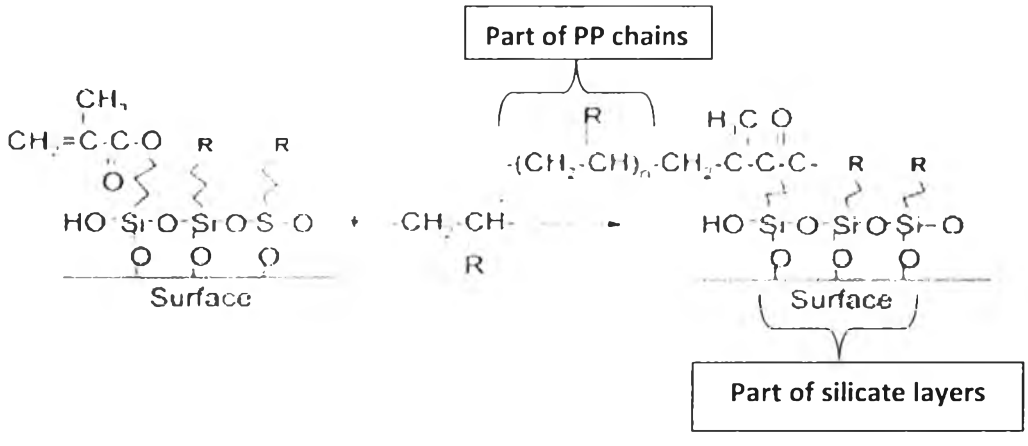

(b)

Figure 4.7 (a) Schematic diagram of surface modification by silanation with MPS and (b) Schematic representative of grafting reaction of polymer onto a silane-treated clay.

Figure 4.8 (a) shows the FTIR spectra of all the xylene-soluble fractions. The spectra mainly showed the characteristic peaks of PP, yet certain weak signals in the rage of 600 – 400 cm^{-1} and at 1041 cm^{-1} also confirmed the presence of trace amount of the inorganic filler in these fractions (Muksing, 2011). In the case of

the residue fractions (Figure 4.8 (b)), the FTIR spectra illustrated the characteristic peaks both of the PP and bentonite. The absorption peak at 3426 was assigned to –OH stretching of lattice water (Muksing, 2011). The medium sharp band at 915 and 845 cm^{-1} are assigned to Al—Al—OH and Al—Mg—OH bonds, respectively (Żymankowska-kumon *et al.*, 2012). The absorption bands at 599 and 526 cm^{-1} are because of Al–O–Si bending vibrations (Żymankowska-kumon *et al.*, 2012) as well as the sharp band at 463 cm^{-1} is attributed to Si–O–Si bending vibrations (Zhirong *et al.*, 2011). The very strong absorption band at 1040 cm^{-1} is due to Si–O bending vibration (Rodriguez *et al.*, 1999). Meanwhile, the characteristic peaks of PP appeared at around 3000 – 2800 cm^{-1} corresponded to the stretching vibrations of aliphatic hydrocarbon (CH bonds; CH_3 and CH_2). Moreover, peaks at 1459 (—CH_3 asymmetry stretching), 1377 (—CH_3 symmetry bending), 1166 (—CH_3 rocking), 973 (—CH_2 rocking), 941 (—CH_3 rocking and C—C stretching), 841 (—CH_2 rocking), and 808 cm-1 (—CH_2 rocking) were attributed to the characteristic peaks of PP (He *et al.*, 2003; Sevegney *et al.*, 2005; Muksing, 2011).

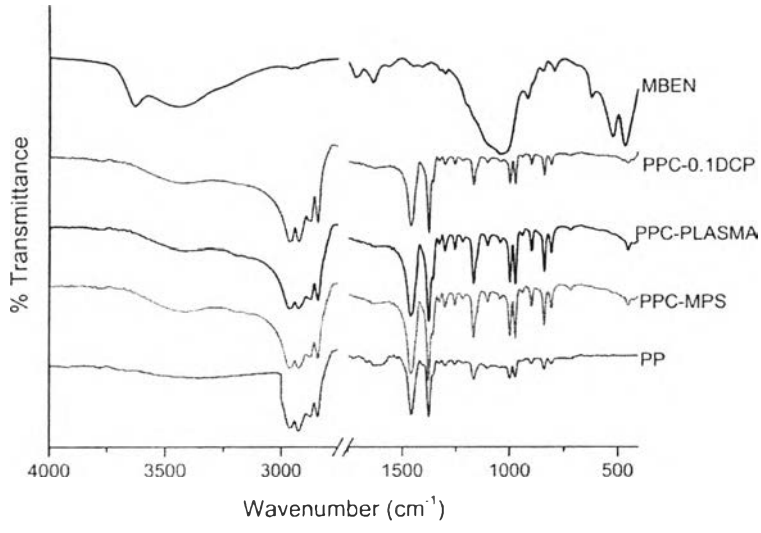

(a) Extraction soluble.

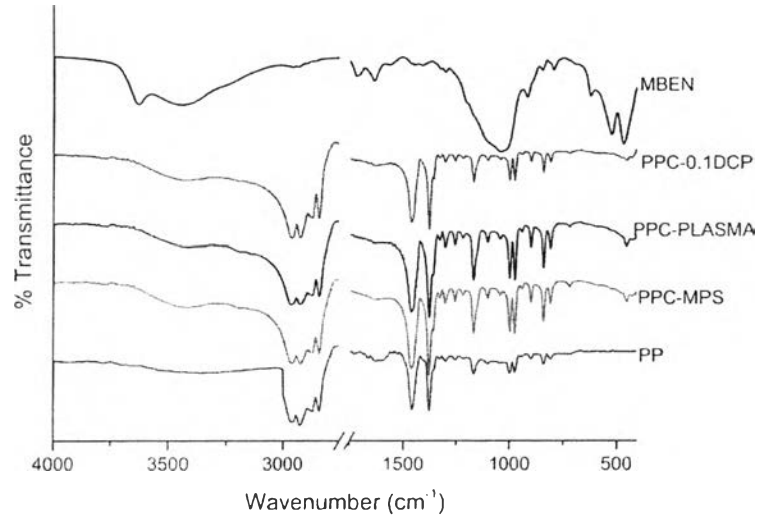

(b) Extraction residue.

Figure 4.8 FTIR spectra of the (a) soluble fractions and (b) residue portions of neat PP and PP-clay nanocomposites fabricated by different methods, as well as modified bentonite.

From the Table 4.5, it was noticed all the nanocomposites gave the higher contents of residues in the thimble than that of neat PP. Still, with the reactive processing, PPC-PLASMA and PPC-0.1DCP provided the greater amounts of residues than that of the nanocomposite without a reactive step (PPC-MPS). This implied that the reactive extrusion generated the grafting between the layered silicate and polymer (Tassanatanachai and Magaraphan, 2007). It was obviously that the PPC-PLASMA gave the highest amount of residue compared to those of neat PP and the other nanocomposites. This implied the strong interaction between the inorganic filler and polymer matrix. It was also confirmed by the highest shift to higher temperature of T_g of the residue from -44.7 °C (T_g of neat PP) to 43.2 °C (T_g of PPC-PLASMA), which indicated the extraction rendered the residue comprising of mostly polypropylene-intercalated bentonite. Passaglia et al., 2008 suggested that the increasing T_g of the residue was able to agree with the confinement effect of the polymer chains between the silicate layers. Their strong interplay was further confirmed by TGA analysis. In the case of residue of PPC-PLASMA, its onset degradation temperature was greater than those of other residues, and it was evidently seen at 2 wt% loss, the residue had T_d higher than virgin residue of PP approximately 7.5 °C. Moreover, the residue of PPC-PLASMA presented the highest amount of char residue at 900 °C. Therefore, the residue of PPC-PLASMA possessed of the highest thermal stability.

Table 4.5 Xylene extraction results, T_g, T_m, T_d, and char residue of pure PP, PPC-MPS, PPC-PLASMA, and PPC-DCP

Material	Xylene-soluble (wt% ungrafted)[a]	Xylene-residue (wt% grafted)[b]	T_g (°C)[c]	T_m (°C)[d]	T_d Onset (°C)[e]	T_d @2wt%loss (°C)[f]	Char @900°C (wt%)[g]
PP	74.45	25.55	-47.7	159.9	438.5	395.0	0
PPC-MPS	64.35	35.65	-44.1	160.7	439.8	386.8	0.2
PPC-PLASMA	43.58	56.42	-43.2	162.8	441.4	402.5	2.1
PPC-0.1DCP	45.84	54.16	-46.2	160.4	439.0	395.4	1.8

[a] Soluble fraction to the extraction with boiling xylene in a Soxhlet extraction for 24 hr calculated as percentage of starting material

[b] Residue fraction to the extraction with boiling xylene in a Soxhlet extraction for 24 hr calculated as percentage of starting material

[c] Glass transition temperature (T_g) of the xylene-residue fractions of nanocomposites calculated in the range of -50 °C and -10 °C in the second heating curve from DSC experiment

[d] Melting temperature (T_m) of the xylene-residue fractions of nanocomposites calculated in the range of 0 °C and 200 °C in the second heating curve from DSC experiment

[e] Decomposition temperature at the onset of nanocomposite degradation recorded in the range from 30 °C to 900 °C obtained from the TGA curve

[f] Decomposition temperature at the 2 wt% loss of nanocomposite degradation recorded in the range from 30 °C to 900 °C obtained from the TGA curve

[g] Char residue at 900 °C for the xylene-residue fraction obtained from TGA analysis

4.5 Conclusions

The bentonite was successfully modified by γ-MPS (MPS–Bentonite) prior to mixing with PP, confirmed by FTIR spectra. It was found that the new bands of functional groups occurred after treatment. From XRD patterns, the increasing of basal spacing indicated the organosilane partly intercalated to the clay intergalleries. TGA thermograms further showed the amount of silane adsorbed on the clay surface was around 8.81 %.

In the case of PP-clay nanocomposites, after adding 5 wt.% of modified clay, the FE-SEM/EDS mapping revealed that the performance of plasma provided the good distribution and dispersion of clay in the PP matrix rather than the chemical initiator did in this study. Meanwhile, the XRD pattern showed the partially intercalated PP chain into the interlamellar space of bentonite. Simultaneously, it was clearly seen that the decomposition temperature of the plasma treated nanocomposite increased most compared to that of virgin PP as a result of the presence of organosilane-modified clay with good layer delamination and distribution.

To investigate the interfacial interaction between PP and modified clay, the solvent extraction by boiling xylene was carried out. It was found that the residue of PPC-PLASMA rendered the highest of weight percentage of residue, shift of T_g to higher temperature, thermal stability, and char residue at 900 °C, which implied the robust interaction between polymer chains and silicate layers.

In summary, the significant changes on the morphology and thermal stability of PP-clay nanocomposites were not only affected by the incorporation of modified clay, but also affected by the different preparation approaches of nanocomposites. Finally, this research also exhibits the one-step fabrication which provides a novelly versatile concept for polymer-clay nanocomposites manufacturing by direct melt intercalation equipped with plasma generator and importantly no requirement for compatibilizers.

4.6 Acknowledgements

This work was financially supported by the Higher Education Research Promotion and National Research University Project of Thailand, Office of the Higher Education Commission (FW0649A). The author is grateful for chemicals and the laboratory equipment support from Polymer Processing and Polymer Nanomaterials Research Unit, The Petroleum and Petrochemical College, Chulalongkorn University.

4.7 References

Azizi, H., Morshedian, J., Barikani, M., Wagner, M.H. (2010) Effect of Layered Silicate Nanoclay on the Properties of Silane Crosslinked Linear Low-Density Polyethylene (LLDPE). eXPRESS Polymer Letters, 4, 252–262.

He, J. D., Cheung, M.K., Yang, M. S., Qi, Z. (2003) Thermal Stability and Crystallization Kinetics of Isotactic Polypropylene/Organomontmorillonite Nanocomposites. Journal of Applied Polymer Science, 89, 3404-3415.

Joo, J. H., Shim, J. H., Choi, J. H., Choi, C.-H., Kim, D.-S., Yoon, J.-S. (2008) Effect of the Silane Modification of an Organoclay on the Properties of Polypropylene/Clay Composites. Journal of Applied Polymer Science, 109, 3645-3650.

Kim, E. S., Shim, J. H., Woo, J. Y., Yoo, K. S., Yoon, J. S. (2010) Effect of the Silane Modification of Clay on the Tensile Properties of Nylon 6/Clay Nanocomposites. Journal of Applied Polymer Science, 117, 809-816.

Li, J., Zhou, C.X., Wang, G., Zhao, D.L. (2003) Study on Rheological Behavior of Polypropylene/Clay Nanocomposites. Journal of Applied Polymer Science 89, 3609-3617.

Liu, X.-L., Han, Y., Gao, G., Li, Z.-Y., Liua, F.-Q. (2008) Effect of Silane Coupling Agent on the Mechanical, Thermal Properties and Morphology of Tremolite/PA1010 Composites. Chinese Journal of Polymer Science, 26, 255-262.

Maria, A. D., Aurora, A., Montone, A., Tapfer, L., Pesce, E., Balboni, R., Schwarz, M., Borriello, C. (2011) Synthesis and Characterization of PMMA/Silylated MMTs. Journal of Nanoparticle Research, 13, 6049-6058.

Marquez, M., Grady, B. P., Robb, I. (2005) Different Methods for Surface Modification of Hydrophilic Particulates with Polymers. Colloids and Surfaces A: Physicochemical and Engineering Aspects, 266, 18-31.

Mishra, S. B., Luyt, A. S. (2008) Effect of Organic Peroxides on the Morphological, Thermal and Tensile Properties of EVA-Organoclay Nanocomposites. eXPRESS Polymer Letters, 2, 256-264.

Muksing, N. (2011) Modification of Layered Silicates and Layered Double Hydroxides for Preparation of Polyolefin Nanocomposites. Ph.D. Thesis, The Petroleum and Petrochemical College, Chulalongkorn University, Thailand.

Nehra, V., Kumar, A., Dwivedi, H.K. (2008) Atmospheric Non-Thermal Plasma Sources. International Journal of Engineering, 2, 53-68.

Passaglia, E., Bertoldo, W., Ciardelli, F., Prevosto, D., Lucchesi, M. (2008) Evidences of Macromolecular Chains Confinement of Ethylene-Propylene Copolymer in Organophilic Montmorillonite Nanocomposites. European Polymer Journal, 44, 1296-1308.

Passaglia, E., Bertuccelli, M., Ciardelli, F. (2001) Composites from Functionalized Polyolefins and Silica. Macromolecular Symposia, 176, 299-315.

Ray, S.S., Okamoto, M. (2003) Polymer/Layered Silicate Nanocomposites: A Review from Preparation to Processing. Progress in Polymer Science, 28, 1539-1641.

Rodriguez, M. A., Liso, M. J., Rubio, F., Rubio, J., Oteo, J. L. (1999) Study of the Reaction of Gamma-Methacryloxypropyltrimethoxysilane (Gamma-MPS) with Slate Surfaces. Journal of Materials Science, 34, 3867-3873.

Sevegney, M. S., Kannan, R. M., Siedle, A. R., Percha, P. A. (2005) FTIR Spectroscopic Investigation of Thermal Effects in Semi-Syndiotactic Polypropylene. Journal of Polymer Science: Part B: Polymer Physics, 43, 439–461.

Sharma, S.K., Nayak, S.K. (2009) Surface Modified Clay/Polypropylene (PP) Nanocomposites: Effect on Physico-Mechanical, Thermal and Morphological Properties. Polymer Degradation and Stability, 94, 132-138.

Sun, Y.-Y., Chen, C.-H. (2007) PMMA/Montmorillonite Nanocomposites by Bulk Polymerization: Mechanical and Thermal Properties. Online Proceedings of the 16th International Conference on Composite Materials (ICCM), Kyoto, Japan.

Tang, Y., Hu, Y., Song, L., Zong, R., Gui, Z., Chen, Z., Fan, W. (2003) Preparation and Thermal Stability of Polypropylene/Montmorillonite Nanocomposites. Polymer Degradation and Stability, 82, 127–131.

Tasanatanachai, P., Magaraphan, R. (2007), Polystyrene/Plasma Treated Clay Nanocomposite. Solid State Phenomena, 121-123, 1493-1496.

Varothai, Y. (2007) Active Packaging Based on Ethylene Scavenger PP/ Organomodified Clay Nanocomposites. M.S. Thesis, The Petroleum and Petrochemical College, Chulalongkorn University, Thailand.

Wan, C., Bao, X., Zhao, F., Kandasubramanian, B., Duggan, M.P. (2008) Morphology and Properties of Silane-Modified Montmorillonite Clays and Clay/PBT Composites. Journal of Applied Polymer Sciences, 110, 550-557.

Wang, K., Chen, L., Kotaki, M., He, C. (2007) Preparation, Microstructure and Thermal Mechanical Properties of Epoxy/Crude Clay Nanocomposites. Composites Part A: Applied Science and Manufacturing, 38, 192-197.

Xie, Y., Hill, C.A.S., Xiao, Z., Militz, H., Mai, C. (2010) Silane Coupling Agents Used for Natural Fiber/Polymer Composites: A Review. Composites Part A: Applied Science and Manufacturing, 41, 806-819.

Zhirong, L., Uddin, M. A., Zhanxue, S. (2011) FT-IR and XRD Analysis of Natural Na-Bentonite and Cu(II)-Loaded Na-Bentonite. Spectrochimica Acta Part A: Molecular and Biomolecular Spectroscopy, 79, 1013–1016.

Żymankowska-Kumon, S., Holtzer, M., Olejnik, E., Bobrowski, A. (2012) Influence of the Changes of the Structure of Foundry Bentonites on Their Binding Properties. Materials Science, 18, 57-61.